

Investigation of effect of x in $\text{Yb}_{1-x}\text{Gd}_x\text{Ba}_2\text{Cu}_3\text{O}_{7-y}$ superconducting structures on upper critical magnetic field and coherence length

This content has been downloaded from IOPscience. Please scroll down to see the full text.

2009 J. Phys.: Conf. Ser. 153 012007

(<http://iopscience.iop.org/1742-6596/153/1/012007>)

View [the table of contents for this issue](#), or go to the [journal homepage](#) for more

Download details:

IP Address: 95.183.245.177

This content was downloaded on 05/05/2015 at 12:24

Please note that [terms and conditions apply](#).

Investigation of effect of x in $\text{Yb}_{1-x}\text{Gd}_x\text{Ba}_2\text{Cu}_3\text{O}_{7-y}$ superconducting structures on upper critical magnetic field and coherence length

Ş. Çelik¹, K. Öztürk² and E. Yanmaz²

¹ Rize University, Faculty of Arts and Sciences, Department of Physics, Rize, Turkey.

² Karadeniz Technical University, Faculty of Arts and Sciences, Department of Physics, Trabzon, Turkey.

E-mail: sukrucelik@yahoo.com

Abstract. The resistivity measurements of the $\text{Yb}_{1-x}\text{Gd}_x\text{Ba}_2\text{Cu}_3\text{O}_{7-y}$ superconducting samples prepared by using the solid-state reaction technique for $x=0.0, 0.2, 0.4, 0.6, 0.8$ and 1.0 were performed in QD-PPMS system under different magnetic fields up to 5T in zero field cooling regime. The upper magnetic field $H_{c2}(T=0)$ for each sample was calculated from 50% of the normalized resistivity (R_n) by the extrapolation $H_{c2}(T)$ to $T=0\text{K}$ and the coherence lengths $\xi(T=0)$ of the samples were calculated from the $H_{c2}(0)$ values. The examination of the effects of x in the composition on $H_{c2}(0)$ showed us that the upper critical magnetic field decreased from 186.31T for $x=0.0$ to 37.99T for $x=1.0$ with the increasing of content x from $x=0.0$ to 1.0 . Using the content x in the composition, the upper critical magnetic field can be controlled and this can be used in superconducting application especially as a superconducting relays.

1. Introduction

Superconducting materials, such as YBCO and BSCCO, must operate at high currents and magnetic fields for many practical applications. Typical large scale applications of them are magnets, power transmission lines, transformers and generators because superconductors have smaller power losses compared to the metals. For these applications, one of the important properties of the superconducting materials is the upper critical magnetic field. The upper critical magnetic field $H_{c2}(0)$ that the material keep its superconductivity is the huge magnetic field at zero temperature for that material. In the higher magnetic field than $H_{c2}(0)$, the material loses its superconductive properties at zero temperature. Many of the studies up to now have been on the development of the transition temperature T_c , $H_{c2}(0)$ and the critical current density J_c of the superconducting structures.

Some researchers studied the effects of the substitution of the rare earth atom with Y in the polycrystalline or crystal superconducting structure of $\text{YBa}_2\text{Cu}_3\text{O}_7$ (Y123). In the studies, the substitution of RE atoms (RE: Nd, Sm, Eu, Gd) in RE123 structure showed that they are effective in achieving high value of critical current density (J_c) in a high magnetic field region accompanied by the secondary peak effect [1]. While the substitution of rare earth atoms (except Ce, Pr, Tb, Pm) for Y in $\text{YBa}_2\text{Cu}_3\text{O}_{7-y}$ (Y-123) preserves the 90K superconductivity [2], the same substitution changes the critical current density J_c and the upper critical magnetic field H_{c2} . One of the factors affecting J_c and H_{c2} is the fabrication processes such as calcinating and sintering processes [3]. When the sintering temperature of the superconducting structure is taken very lower than the peritectic decomposition temperature, the structure has the weak-link interaction or its superconductivity disappear. While the strong and weak interactions in the same superconducting sample are under control, the upper critical magnetic field of the sample can be assigned at the desired value in the specific range of magnetic field which is possible.

Our previous study was about the effects of content x in $\text{Y}_{1-x}\text{Yb}_{x/2}\text{Gd}_{x/2}\text{Ba}_2\text{Cu}_3\text{O}_7$ (Y, Yb, Gd)123 structure on the upper critical magnetic field and coherence length [10]. It was found in our previous study that Yb123 phase in this composition has stronger interactions and Gd123 has weaker interactions compared to Y123. Owing to three interactions in the structure, the upper critical magnetic field was changed from 84T to 122T with the content x .

¹ Corresponding author: e-mail: sukrucelik@yahoo.com, Phone: +90 4642236126, Fax: +90 4642235376.

In this study, we investigated the effect of Gd123 and Yb123 structures without Y123 phase in the superconducting material of $\text{Yb}_{1-x}\text{Gd}_x\text{Ba}_2\text{Cu}_3\text{O}_7$ (Yb, Gd)123 for $x=0.0, 0.2, 0.4, 0.6, 0.8$ and 1.0 . Because the peritectic decomposition temperature of Gd123 structure is 975°C [4] and Yb123 is 910°C [5], the sintering temperature of the sample was selected as 890°C to fabricate Yb123 with strong interaction and Gd123 with weak interaction in the same composition. Using the content x , the amounts of both interactions were thought to change and to control upper critical magnetic field of the sample.

Although numerous studies have been undertaken on the pinning properties of melt processed Yb123 [6] with finely dispersed Y211, the effect of x in $\text{Yb}_{1-x}\text{Gd}_x\text{Ba}_2\text{Cu}_3\text{O}_7$ polycrystalline structure on the activation energy and the c -lattice parameter [7, 8], the effect of x of $\text{Y}_{1-x}\text{Gd}_{x/2}\text{Yb}_{x/2}\text{Ba}_2\text{Cu}_3\text{O}_7$ superconducting structures on the activation energy [9] and the upper critical magnetic field [10], the effect of Gd diffusion into Y123 [11, 12], and Yb diffusion into Y123 [13], no studies on the effect of x in such $\text{Yb}_{1-x}\text{Gd}_x\text{Ba}_2\text{Cu}_3\text{O}_{7-y}$ polycrystalline superconducting structure on the upper critical magnetic field and the coherence length have been reported.

2. Experimental

The polycrystalline $\text{Yb}_{1-x}\text{Gd}_x\text{Ba}_2\text{Cu}_3\text{O}_{7-y}$ ((Yb, Gd)123) superconducting samples were produced by solid state reaction method for the six different x values. After stoichiometric mixtures of Yb_2O_3 , Gd_2O_3 , BaCO_3 and CuO for each composition of x were thoroughly ground and calcined at 900°C in air for 10 h, each mixture was ground again, and pressed into a pellet form with 13mm diameter under 250 MPa pressure, and then each of the samples for $x=0, 0.2, 0.4, 0.6, 0.8$ and 1 was sintered at 890°C for 24h in air. Finally, all the samples together were subjected to oxygenation process at 400°C for 2h, followed to 300°C at the rate of $-1^\circ\text{C}/\text{min}$ under the oxygen flowing and then they were cooled to the room temperatures in air. Samples were cut into bar-shape with identical dimensions with the size of $1.5 \times 2.0 \times 6.0 \text{ mm}^3$. The sintering and oxygenation temperatures of the samples were obtained from the Differential Thermal Analysis (DTA) model NETZSCH1.

The standard four-probe resistivity of samples were measured by using a physical properties measurement system (Quantum Design PPMS system) under various magnetic fields such as 0, 1, 2, 3, 4 and 5T in the zero field cooling regime (ZFC). In order to remove the trapped magnetic field inside the samples, 0.1T magnetic field was applied for a short time at 100K and then decreased to zero field before ZFC regime.

3 Results and Discussions

The measurements of $H_{c2}(T)$ for the HTSCs have been limited to temperatures near T_c because H_{c2} in these materials rapidly exceeds accessible laboratory magnetic fields when the temperature is reduced to only nine-tenths of T_c [14]. Thus the values of $H_{c2}(0)$ and $\xi(0)$ can be calculated from such data require either a large extrapolation to $T=0\text{K}$ using a presumed functional form for H_{c2} or calculation of H_{c2} from the slope $(dH_{c2}/dT)_{T_c}$ [15] using the Werthamer-Helfand-Hohenberg (WHH) expression $H_{c2}(0)=0.7T_c(dH_{c2}/dT)_{T_c}$ [14]. In this paper, the extrapolation method was used to calculate $H_{c2}(0)$.

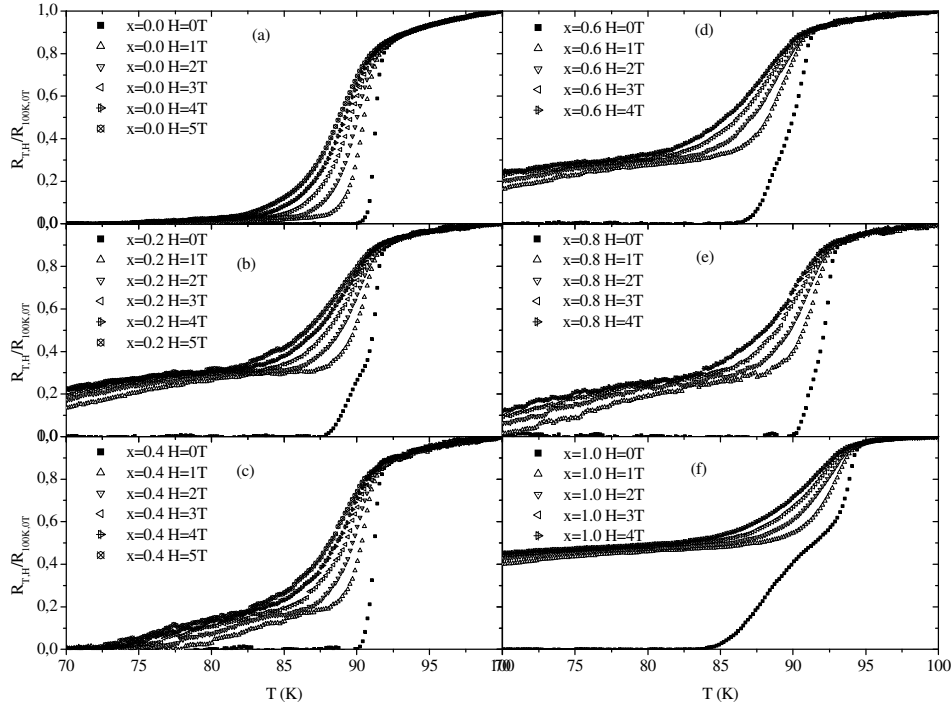


Figure 1. Shows the normalized resistivity versus temperature plots under different magnetic fields up to 5T for the sample a) $x=0.0$, b) $x=0.2$, c) $x=0.4$, d) $x=0.6$, e) $x=0.8$ and f) $x=1.0$

Using the R-T plots in Figure 1, of which the detailed explanations were given in our previous paper in ref [7], the upper critical magnetic field can be calculated from the expression below [16, 17]:

$$H_{c2}(T) = \frac{\Phi_0}{2\pi\xi^2(T)} \quad (1)$$

Where Φ_0 is the flux quantum ($\Phi_0=2,067833636 \times 10^{-15} \text{Tm}^2$), and $\xi(T)$ is the coherence length at the temperature T [16, 17]. The dependency of ξ on temperature is given by:

$$\xi(T) = \xi_0 \left(1 - \frac{T_c}{T}\right)^{-1/2} \quad (2)$$

Where ξ_0 is the coherence length ($\xi(0)$) at the temperature of $T=0\text{K}$. When the Equation (2) is replaced with ξ in the Equation (1), the upper critical magnetic field at temperature close to T_c can be rewritten as below:

$$H_{c2}(T) = H_{c2}(0) \left(1 - \frac{T}{T_c}\right) \quad (3)$$

In the expressions, $H_{c2}(T)$ and $H_{c2}(0)$ is the upper critical magnetic field at T and $T=0\text{K}$, respectively. The Equation (3) can be rewritten as follow:

$$H_{c2}(T) = H_{c2}(0) - H_{c2}(0) \frac{T}{T_c} \quad (4)$$

There are some ideas in previous researchers to define the transition temperature T in the Equation (4). In the study of Müller and his friends [19], they used the magnetic field and the temperature values (as H_{10} , H_{50} and H_{90}) were defined when the resistance of the sample is 10, 50 and 90% of the normal-state resistance R_n , respectively. After the comparison of the upper critical magnetic fields of 10, 50 and 90% of R_n with the fields obtained from dc magnetization and ac susceptibility measurements, they showed us that H_{90} agrees with the result obtained from magnetization, whereas H_{c2} which determined from susceptibility coincides with the H_{10} for MgB_2 . On the other hand, in the study of Ando and his friends [18], they associated H_{50} with the mean-field upper critical magnetic field H_{c2} .

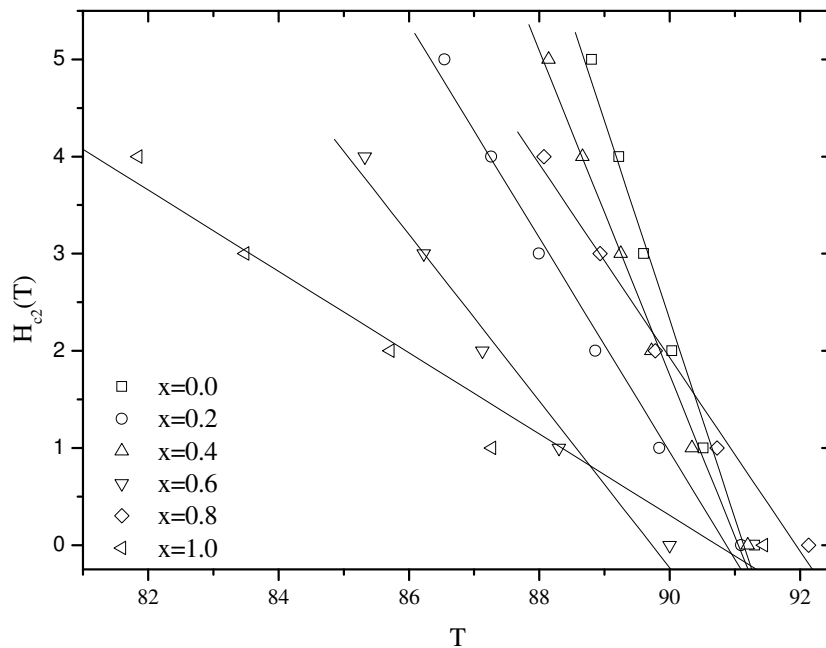


Figure 2. Shows the $H_{c2}(T)$ versus $T_c(H)$ calculated from R-T plots for the samples under different magnetic fields.

In this paper, we calculated the upper critical magnetic field such as $H_{c2}(T)$ and T values at which the normalized resistivity equal to 50% of R_n using the R-T plots in Figure 1, and $H_{c2}(T)$ versus T plots were shown in Figure 2. In this figure, each dot corresponds to the upper critical magnetic field for the samples at the different critical transition temperature T_c under different applied magnetic fields. After the linear fittings of the plots in Figure 2, $H_{c2}(0)$ values for the samples were calculated using the extrapolation of $H_{c2}(T)$ to $T=0K$. $H_{c2}(0)$ versus content x was shown in Figure 3.

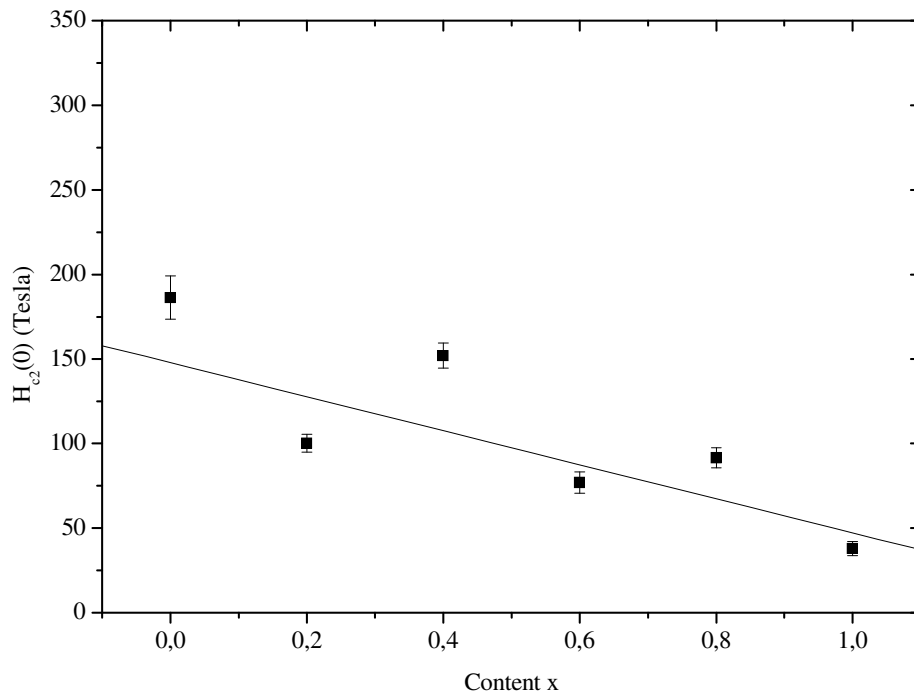


Figure 3. Shows $H_{c2}(0)$ values versus content x. Solid line in the plot is the linear fitting.

When the Figure 3 was generally examined, it was resulted that the value of the $H_{c2}(0)$ is roughly decreasing with the increasing of the content x. While content x is increasing, not only is the amount of content Yb decreasing, but also that of content Gd is increasing. So, it is resulted in decreasing of $H_{c2}(0)$ value with increasing of content x. This says us that Yb123 structure is more resistive than Gd123 structure against to the higher magnetic fields in this study. In fact, this is not unusual result of Gd123 structure due to the sintering temperature. Because Yb123 liquidation temperature which is 910°C [5], the sintering temperature of the composition was estimated as 890°C and also this is very low sintering temperature for Gd123 structure. While this temperature is very suitable for Yb123, it is also near enough below sintering temperature of Gd123 structure. The decreasing of $H_{c2}(0)$ with the increasing of the content x shows us that this sintering temperature resulted the weak interaction between grains in Gd123 and also strong interaction in Yb123 structures.

The separation from the linearity in the plot in Figure 3 is thought to originate from the extrapolations which are used to calculate $H_{c2}(0)$. In the extrapolation of plots in Figure 3 to calculate $H_{c2}(0)$, only five different magnetic fields up to 5T were used. Higher magnetic fields than 5T is not possible in our laboratory. On the other hand, when the Figure 3 is examined, it is clear to be seen that the strongest structure against to the magnetic field is $x=0.0$, corresponding to Yb123, and the weakest one is $x=1.0$, corresponding to Gd123 structure. While the $H_{c2}(0)$ value of Y123 thin single superconducting crystal sample with $B \parallel c$ and $B \perp c$ are 250 T and 120 T respectively [20], that value for our polycrystalline superconducting samples in this study is decreasing from 186 T to 38 T with the increasing of content x. Indeed, the upper critical magnetic field of Gd123 is not around 38 T and more much than 38 T. But, we had to estimate the sintering temperature as 890 °C to apply the same sintering tem-

perature for all the samples in this study. We aimed to produce the sample which has Yb123 superconducting structure with the strong interaction and Gd123 with the weak interaction between grains. This temperature produced Gd123 with very weak-link interaction in the composition as low as it can keep its superconductivity, on the other side, produced Yb123 with very strong interaction. The effects of both structures in the same composition in this study resulted in the variation of the upper critical magnetic field from 186T to 38 T. While the strong interaction tries to make H_{c2} of the sample to be higher, the weak interaction does it to be lower. The greatneses of two interactions are originated from the quantities of Yb123 and Gd123 structures in the composition. Because these quantities are related to x , the content x can be used to control the upper critical magnetic field. This idea can be understood from the Figure 3. In the figure, there is nearly linear decreasing with the increasing of the content x .

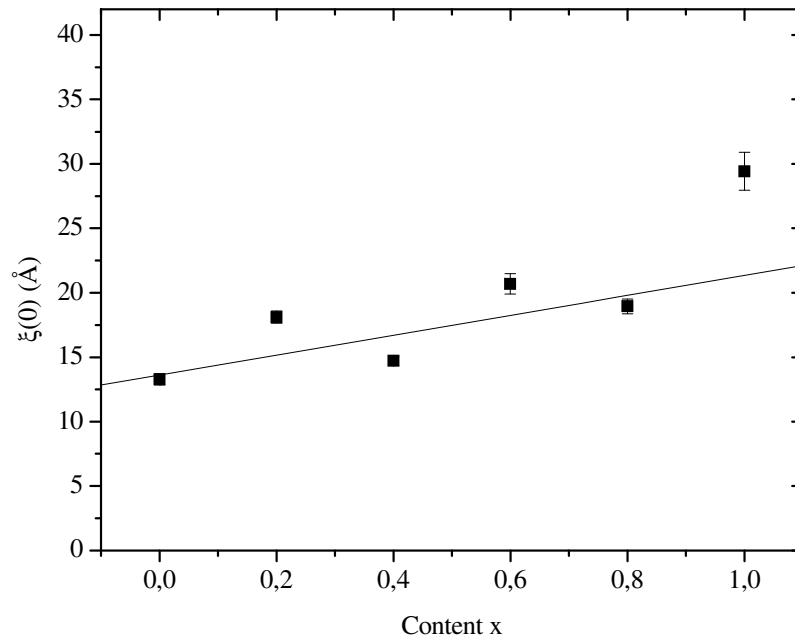


Figure 4. Shows the coherence length $\xi(0)$ versus content x . Solid line in the plot is the linear fitting.

As for the coherence length ξ , it is one of the characteristic parameters of the superconductors. It is a difficult quantity to measure directly, however, it was thus calculated from the expression $H_{c2}(0) = \Phi_0 / 2\pi\xi^2$ and ξ - content x plot is shown in Figure 4. The coherence length is about 16 Å for $YBa_2Cu_3O_{7-y}$ [21,22], 13.6 Å for Tl-2223 [23,24], 9.7 Å for Bi-2223 and 9 ± 1 Å for Bi-2212 [25], and this value in this study is varying roughly linear from ~ 13 Å to ~ 29 Å with increasing of the content x from $x=0.0$ to $x=1.0$. The coherence length can be controlled by the content x . The separation from the linearity is originated from the separation in $H_{c2}(0)$ versus content x plot in Figure 3.

From the linear fittings of the plots in Figure 3 and Figure 4, the relationships between $H_{c2}(0)$ and $\xi(0)$ with content x and the inverse relations are defined below:

$$H_{c2}(0) = A + B \cdot x \quad (\text{in T}) \quad x \text{ is defined in the range of } 0-1.0 \quad (5a)$$

$$\xi(0) = A' + B' \cdot x \quad (\text{in Å}) \quad x \text{ is defined in the range of } 0-1.0 \quad (5b)$$

$$x = A'' + B'' H_{c2}(0) \quad H_{c2}(0) \text{ is defined in the range of } 38\text{T} - 186\text{T} \quad (6a)$$

$$x = A''' + B''' \xi(0) \quad \xi(0) \text{ is defined in the range of } 13\text{\AA} - 29\text{\AA} \quad (6b)$$

Table 1. The constants used in the Eq(5a, 5b, 6a and 6b) with their errors.

Constant	Value	Error	Constant	Value	Error
A	147.8606	±5.3237	B	-10.0602	±0.7329
A'	13.6241	±0.3387	B'	7.7089	±0.7729
A''	11.3526	±2.2226	B''	-0.0591	±0.0189
A'''	-0.5496	±0.3591	B'''	0.0547	±0.0181

The constants in Equation (5) and Equation (6) are listed in Table 1. Using the content x in $\text{Yb}_{1-x}\text{Gd}_x\text{Ba}_2\text{Cu}_3\text{O}_{7-y}$ structure, and the constants in Table 1, $H_{c2}(0)$ or $\xi(0)$ of the sample with any content x in the range of $x=0.0 - 1.0$ can be calculated from Equation (5a) and Equation (5b) respectively. On the other hand, it can be calculated that which sample with the desired $H_{c2}(0)$ or $\xi(0)$ values in the specific range should have the content x using Equation (6a) and Equation (6b) respectively.

4. Conclusion

Using the standard solid-state-reaction technique, the nominal composition of $\text{Yb}_{1-x}\text{Gd}_x\text{Ba}_2\text{Cu}_3\text{O}_{7-y}$ superconductor samples for $x=0.0, 0.2, 0.4, 0.6, 0.8$ and 1.0 were prepared. The upper critical magnetic field $H_{c2}(T)$ at the temperature $T=T$ for the samples were calculated by the midpoint of the normalized resistivity values obtained from the resistivity measurements in the different magnetic fields up to 5T under zero field cooling regime and the upper critical magnetic field $H_{c2}(0)$ at the temperature $T=0\text{K}$ was found by the extrapolation $H_{c2}(T)$ to $T=0\text{K}$. The coherence length values were calculated by using the upper critical magnetic field values at the temperature $T=0\text{K}$.

The calculations presented us that while the coherence length is 16\AA for Y123, 13.6\AA for Tl2223, 9.7\AA for Bi2223 and $\sim 9\text{\AA}$ for Bi2212, this value in this study varies from $\sim 13\text{\AA}$ to $\sim 29\text{\AA}$ and $H_{c2}(0)$ is varying from 186T to 38T with increasing content x from $x=0.0$ to 1.0 .

In our study it was found that there are two interactions in the composition and they are the strong interaction in Yb123 and the weak interaction in Gd123 structure. The quantities of both interactions were changed with the content x because the amount of Yb123 is decreased and that of Gd123 is increased with the increasing of the content x . The quantities of Yb123 and Gd123 structures in the composition supplied us to control the upper critical magnetic field in the identical range of $37\text{T} - 186\text{T}$. Consequently, using the content x in $\text{Yb}_{1-x}\text{Gd}_x\text{Ba}_2\text{Cu}_3\text{O}_{7-y}$ structure, $H_{c2}(0)$ or $\xi(0)$ of the sample with any content x between $0.0 - 1.0$ can be calculated from the Equation (5a) and Equation (5b) respectively. On the other hand, it can be calculated that which sample with the desired $H_{c2}(0)$ or $\xi(0)$ values in the specific range should have the content x using Equation (6a) and Equation (6b) respectively. By this way, we don't need to produce and measure the sample with any other content x in the range of $0.0 - 1.0$ to find $H_{c2}(0)$ and $\xi(0)$. In addition, this study showed us that the upper critical magnetic field can be controlled using the content x in our compositions and this controlling of the upper critical magnetic field can be used in the application of superconductivity as an electronic superconducting switches.

References

- [1] Murakami M 1992 *Supercond. Sci. Technol.* **5** 185
- [2] Tarascon J M, McKinnon W R, Greene L H, Hull G W and Vogel E M 1987 *Phys. Rev. B* **36** 26

- [3] Yamani Z and Akhavan M 1997 *Supercond. Sci. Technol.* **10** 427
- [4] Nariki S, Sakai N, Inoue K and Murakami M, 2003 *Physica C* **392** 468
- [5] Won C, Kinder L R, Gim Y, Fan Y, Coulter J Y, Maley M P, Foltyn S R, Peterson D E and Jia Q X, 1999 *Appl. Supercond.* **9** (2) 1575
- [6] Mochida T, Sakai N, Yoo S I and Murakami M, 2002 *Physica C* **366** 229
- [7] Çelik Ş, Öztürk K and Yanmaz E, 2008 *J. Alloys Compd.* **456** 1
- [8] Çelik Ş, Thesis Ph D, Karadeniz Technical University, June 2006, Trabzon, Turkey.
- [9] Çelik Ş, Öztürk K, Çevik U and Yanmaz E, 2008 *J. Alloys Compd.* **460** 79
- [10] Çelik Ş, Öztürk K and Yanmaz E, 2008 *J. Alloys Compd.* **458** 30
- [11] Öztürk K, Çelik Ş, Çevik U and Yanmaz E 2007 *J. Alloys Compd.* **433** 46
- [12] Öztürk K, Çelik Ş and Yanmaz E, 2008 *J. Alloys Compd.* **462** 19
- [13] Öztürk K, Çelik Ş, Çevik U and Yanmaz E, 2008 *J. Alloys Compd.* **456** 34
- [14] Osofsky M S, Soulen R J, Wolf S A, Broto J M, Rakoto J M, Ousset J C, Coffe G, Askenazy S, Pari P, Bozovic I, Eckstein J N and Virshup G F, 1993 *Phys. Rev. Lett.* **71** 14
- [15] Helfand E, Werthamer N R and Hohenberg P C, 1966 *Phys. Rev.* **147** 295
- [16] Thinkam M, 1996 *Introduction to Superconductivity*, Second Ed. McGraw-Hill New York 118
- [17] Shigeta I, Abiru T, Abe K, Nishida A and Matsumoto Y, 2003 *Physica C* **392** 359
- [18] Ando Y, Boebinger G S, Passner A, Schn L F, Kimura T, Okuya M, Watauchi S, Shimoyama J, Kishio K, Tamasaku K, Ichikawa N and Uchida S, 1999 *Phys. Rev. B* **60** 17.
- [19] Müller K H, Fuchs G, Handstein A, Nenkov K, Narozhnyi V N and Eckert D, 2001 *J. Alloys Compd.* **322** L10
- [20] Sekitani T, Miura N, Ikeda S, Matsuda Y H and Shiohara Y, 2004 *Physica B* **346** 319
- [21] Welp U, Kwok W K, Crabtree G W, Vandervoort K G and Liu J Z, 1989 *Phys. Rev. Lett.* **62** 1908
- [22] Hao Z, Clem J R, McElfresh M W, Civale L, Malozemoff A P and Holtzberg F, 1991 *Phys. Rev. B* **43** 2844
- [23] Brandstatter G, Sauerzopf F M, Weber H W, Ladenberger F and Schwarzmann E, 1994 *Physica C* **235** 1845
- [24] Thompson J R, Ossandon J G, Christen D K, Chakoumakos B C, Sun Y R, Paranthaman M and Brynstad J, 1993 *Phys. Rev. B* **48** 14031
- [25] Li Q, Suenaga M, Hikata T and Sato K, 1992 *Phys. Rev. B* **46** 5857